Conference on Turbulence and Interactions TI2006, May 29 - June 2, 2006, Porquerolles, France

STRONGLY ANISOTROPIC TURBULENCE, STATISTICAL THEORY AND DNS

C. Cambon[†,*]

[†]Laboratoire de Mécanique des Fluides et d' Acoustique, UMR CNRS 5509, École Centrale de Lyon, 69134 Ecully Cedex, France
[*]Email: claude.cambon@ec-lyon.fr

ABSTRACT

Complete anisotropy of second-order statistics is parametrized in Fourier space, in terms of directional and polarization dependence. This description is shown to be useful to analyze homogeneous anisotropic turbulence, interacting with various body forces and/or in the presence of large-scale 'mean' gradients. As far as possible, both statistical theory, ranging from 'Rapid Distortion Theory' to nonlinear theories including it, and recent, often original, DNS data are investigated. Applications to strongly anisotropic turbulence are surveyed, in a rotating, then in a stably stratified fluid. The cases of homogeneous shear, simplified MHD with external magnetic field, and weakly compressible quasi-isentropic flows are touched upon using the same theoretical approach.

1 INTRODUCTION

To the question, what remains to do in turbulence —from the viewpoint of physical understanding (not only modelling and simulating)—, the responses often mention more investigations of intermittency, anisotropy, and inhomogeneity. The problem is that these three aspects are often intimately connected; in the intermittency-scaling community, for instance, the departure of the exponents of the structure functions from the Kolmogorov law (K41) is often investigated without a clear analysis of the different mechanisms called into play. In this paper, the emphasis will be placed on anisotropy, provisionally ignoring inhomogeneity and intermittency, considering that important classes of flow, e.g. relevant to geophysical applications, are strongly anisotropic. On the other hand, inhomogenity is often not crucial far from boundaries, and anisotropy affects low order statistical moments, the ones which deal with energy spectra and interscale energy transfer (cascade), without need for a precise knowledge of high order moments, which are possibly affected by intermittency.

The domain of HAT (Homogeneous Anisotropic Turbulence) [1–3] is illustrated by turbulent flows subjected to body forces, like Coriolis, buoyancy, Lorentz forces, and/or in the presence of large-scale "mean" velocity or density gradients. In this sense, they are relevant to illustrate turbulence and interactions: interactions with different sources of motion, as buoyancy and inertial acceleration, interactions between different modes of motion, as waves and vortices, interactions between fluid dynamics and electromagnetism, ...

In many cases, the feeling that anisotropy is not very important results from the use of very few, very global, and even irelevant, descriptors. On the one hand, the deviatoric part of the Reynolds stress tensor is used as the unique descriptor of anisotropy in the engineering turbulence community; an important exception is the 'structure-based' modelling introduced by Kassinos *et al.* [4], as we will see later. On the other hand, a refined anisotropic description of the second order structure function is being investigated by some specialists of intermittency and scaling: a rational use of the SO(3) symmetry group allows Arad *et al.* [5] to represent both the dependency on the orientation of the two-point separation vector, and the dependency on different orientations, as transversal or longitudinal, of the velocity increment vector. Unfortunately, all the abovementioned approaches to refined anisotropy result in practice in angular harmonics expansions at very low degree for, e.g. the energy spectrum of turbulence. Another problem is that the strong anisotropy of quasi-homogeneous flows, which provides a very large number of angular harmonics, is often ignored, whereas applications emphazise complex inhomogeneous flows, like jets or boundary layers.

Anisotropy is addressed here as a complete description of the second order spectral tensor $\hat{R}_{ij}(\boldsymbol{k})$, which is the three-dimensional Fourier transform of two-point second order velocity correlations

$$R_{ij}(\boldsymbol{r}) = \langle u_i(\boldsymbol{x}) u_j(\boldsymbol{x}+\boldsymbol{r})\rangle. \qquad (1)$$

Fourier space is only a mathematical convenience. Looking at a scalar quantity, like the three-dimensional energy spectrum $e = (1/2)\hat{R}_{ii}(\boldsymbol{k})$, it is clear that similar scalar harmonics expansions can be done for e and for its counterpart in physical space $(1/2)R_{ii}(\boldsymbol{r})$, anisotropy can be seen as a departure from spherical equipartition in terms of $\boldsymbol{k}$ or $\boldsymbol{r}$ dependency, in spectral or in physical space, respectively. This characterizes the *directional anisotropy*, which is very closed to what called 'dimensionality' by [4]. The anisotropic 'componentality' proprerties of R_{ij} are much more complicated, because the constraint that the velocity field is divergence-free cis expressed in terms of partial derivatives, and even integro-differential relations if mixed velocity-pressure correlations are addressed. In contrast, all these constraints amount to algebraic relations in Fourier space, so that a minimal number of components can be defined for generating the entire spectral tensor. As a result, a general description in terms of directional and polarization anisotropy can be found for arbitrary anisotropy, slightly improving seminal studies by Batchelor [1], Craya [6] and Herring [7]. Details are recalled in the next section.

Once the anisotropy defined in the most general way, it is important to look at its generation by linear and nonlinear dynamics. Linear dynamics can be treated in Fourier space, following basic 'Rapid Distortion Theory' (RDT hereinafter) introduced by Batchelor & Proudman and well advanced by Townsend [8]. Also in agreement with the method rediscovered by applied mathematicians (e.g. Craik & Criminale [9]), the starting point consists of providing the *deterministic* Green's function related to the Euler problem, which is for us the building block, before addressing, in a second step, RDT solutions for statistical quantities, and applications to full nonlinear theories and models. Regarding nonlinear dynamics, the Green's function appears as the natural zeroth order for the response tensor, introduced by Kraichnan and present in all subsequent renormalized perturbation theories. A general strategy is proposed to fill the gap between the linear solution and a typical nonlinear theory. The pivotal model, called EDQNM3, is a generalized EDQNM (Eddy Damped Quasi-Normal Markovian [10]) model, in which the so called 'Markovianization' is based upon a rational timescale separation between the 'rapid' effect of the Green's function and the 'slow' evolution of a new set of dependent variables, which are constant in the RDT limit. The eddy damping (ED) is not specified a priori in the model, it is considered as a scalar renormalization of the Green's function, and therefore corresponds to a nonlinear adjustment of the zeroth order response tensor. If the linear effect consists of dispersive waves, the Eulerian Wave-Turbulence theory appears as a limiting case of EDQNM3, with eddy damping (ED) unimportant. In this sense, physically relevant ED allows us to discriminate 'weak' (WT) from 'strong' turbulence : only in the case of strong turbulence, is ED important and must be evaluated by comparison with a more sophisticated self-consistent theory. For instance, The LRA (Kaneda [11] and references therein) is chosen at the end of the list of more and more sophisticated models/theories as follows:

RDT $\subset$ WT $\subset$ EDQNM3 $\subset$ LRA.

The originality of our approach which respect to the ones based on LRA by Kaneda [12] in the same conference, is that no approximation of weak anisotropy is made.

The above mentioned strategy will be illustrated by different cases:

- Pure rotation (section 4).
- Stable stratification with and without rotation (section 5)
- Homogeneous shear flow (section 6)
- MHD turbulence with external magnetic field (section 7)
- Weakly compressible quasi-isentropic isotropic turbulence, with or without mean shear (section 8)

2 Description of Homogeneous Anisotropic Turbulence

As discussed before, arbitrary anisotropy is easier to describe for the second-order spectral tensor $\hat{R}_{ij}(\boldsymbol{k}, t)$, which is the Fourier transform of the correlation tensor in eq. (1). The antisymmetric, purely imaginary, part of the spectral tensor can be related to a scalar helicity spectrum, denoted $\mathcal{H}$, or

$$\frac{1}{2}\left(\hat{R}_{ij} - \hat{R}_{ji}\right) = \imath\epsilon_{ijn}\frac{k_n}{k}\mathcal{H}(\boldsymbol{k}).$$

(the time variable will be omitted from now on, except in some dynamical equations. The spatial variables $\boldsymbol{x}$ or $\boldsymbol{k}$ may also be omitted, for the sake of brevity). This helicity contribution is irrelevant in many cases of homogeneous turbulence, since it cannot be created by the interaction process, so that it would be present only from initial data. ignoring it, as we shall do in this paper unless explicitly stated otherwise, we will only consider $\hat{R}_{ij}$ as symmetric and real. Because of incompressibility, assumed here with the only exception of section 8, $k_i\hat{R}_{ij} = 0$, so that $\hat{R}_{ij}$ can be restricted to a plane normal to $\boldsymbol{k}$. Accordingly, a simple decomposition in terms of trace and deviator can be written as

$$\hat{R}_{ij} = eP_{ij} + \hat{R}^{pol}_{ij}$$

in which $e = \frac{1}{2}\hat{R}_{nn}$, the transverse projection operator

$$P_{ij} = \delta_{ij} - \frac{k_i k_j}{k^2} \qquad (2)$$

playing the role of the identity matrix *restricted to the plane normal to* $\boldsymbol{k}$. The deviatoric part is called 'polarization' with superscript 'pol', as clarified further. Half the trace of the spectral tensor corresponds to the 3D density of spectral energy e, it can be split into a purely isotropic part $U(k)$, which only depends on the wavevector modulus, and a complementary part, denoted $\mathcal{E}(\boldsymbol{k})$, which expresses the departure from spherical equidistribution and generates 'directional' anisotropy. Finally, the polarization part can be related to a complex parameter Z, so that

$$\hat{R}_{ij} = \underbrace{U(k)P_{ij}}_{\text{isotropic}} + \underbrace{\mathcal{E}(\boldsymbol{k})P_{ij}}_{\text{directional}} + \underbrace{\Re\left(Z(\boldsymbol{k})N_iN_j\right)}_{\text{polarization}}. \qquad (3)$$

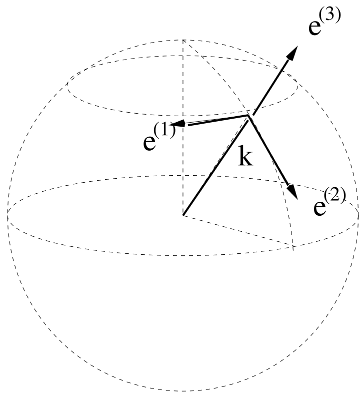

Fig. 1. Craya/Herring frame of reference

Only the polarization term Z and the complex 'helical' vector $\boldsymbol{N}$, which generate the polarization tensor, may depend — only via a unique phase term — on a specific frame of reference in the plane normal to $\boldsymbol{k}$. Choosing for instance a system of tangent vectors in a polar-spherical system of coordinates (unit polar axis $\boldsymbol{n}$, vertical on Fig. 1), one recovers the Craya-Herring frame of reference, defined by

$$\boldsymbol{e}^{(1)} = \frac{\boldsymbol{k}\times\boldsymbol{n}}{\mid \boldsymbol{k}\times\boldsymbol{n}\mid}, \qquad \boldsymbol{e}^{(2)} = \frac{\boldsymbol{k}}{k}\times\boldsymbol{e}^{(1)} \tag{4}$$

if $\mid \boldsymbol{k}\times\boldsymbol{n}\mid\neq 0$ (see Fig. 1) and coinciding with a fixed planar frame if $\boldsymbol{k}\parallel\boldsymbol{n}$. Accordingly, one has

$$P_{ij} = e_i^{(1)}e_j^{(1)} + e_i^{(2)}e_j^{(2)}, \qquad N_i = e_i^{(2)} - \imath e_i^{(1)}.$$

Going back to an intrinsic (frame invariant) representation, $e = U + \mathcal{E}$ is equal to half the sum of the nonzero principal values of the (symmetric real) tensor $\hat{\mathsf{R}}$, the modulus of Z is equal to half their difference, and the phase of Z is connected to the single angle for passing from the Craya-Herring frame to the eigenframe of principal axes by rotation around $\boldsymbol{k}$. The directional anisotropy, quantified by $\mathcal{E}(\boldsymbol{k}) = e(\boldsymbol{k}) - U(k)$, is related to a departure from spherical equidistribution of the 3D density of energy: it means that the different directions of $\boldsymbol{k}$ on a sherical shell of radius $k = \mid \boldsymbol{k}\mid$ are not statistically equivalent regarding energy spectral density. In turn, the polarization anisotropy Z characterizes a lack of statistical invariance with respect to the directions of $\hat{\boldsymbol{u}}$, rotating around $\boldsymbol{k}$, *at a given* $\boldsymbol{k}$.

Of course, the velocity field itself, considered as a random variable in Fourier space, can be expressed in the Craya-Herring frame

$$\hat{\boldsymbol{u}} = u^{(1)}(\boldsymbol{k})\boldsymbol{e}^{(1)} + u^{(2)}(\boldsymbol{k})\boldsymbol{e}^{(2)} \tag{5}$$

or in the basis of helical modes

$$\hat{\boldsymbol{u}} = \xi_{+1}(\boldsymbol{k})\boldsymbol{N} + \xi_{-1}(\boldsymbol{k})\boldsymbol{N}^*, \tag{6}$$

with $\boldsymbol{N}^*(\boldsymbol{k}) = \boldsymbol{N}(-\boldsymbol{k})$ (hermitian property). Simplified relationships for the spectral tensor can be directly obtained from the latter equations by forming $< \hat{\boldsymbol{u}}_i^*\hat{\boldsymbol{u}}_j >$ correlations and using $N_i^*N_j = P_{ij} + \imath\epsilon_{ijn}\frac{k_n}{k}$ and $N_iN_i = 0$.

3 STATISTICAL THEORY AND MODELLING

The case of incompressible turbulence in the presence of space-uniform mean velocity gradients A is chosen below to illustrate the strategy.

3.1 from RDT to EDQNM3

Considering a "disturbance flow" in the presence of a "basic" flow, which is linear in space, solutions are found in term of plane waves with time-dependent wave-vector $\boldsymbol{k}(t)$. Consequently, the disturbance flow is generated by Fourier coefficients, as $\hat{\boldsymbol{u}}(\boldsymbol{k}(t), t)$ for the velocity field $\boldsymbol{u}'(\boldsymbol{x}, t)$, with a simple system of Ordinary Differential Equations (ODE) as

$$\dot{\hat{u}}_i + M_{ij}\hat{u}_j = 0 \tag{7}$$

$$\dot{k}_i + A_{ij}k_j = 0 \tag{8}$$

where A_{ij} is the gradient matrix of the basic flow, and $M_{ij} = (\delta_{in} - 2\frac{k_i k_n}{k^2})A_{nj}$. The 'overdot' denotes a compounded time-derivative accounting for $\boldsymbol{k}(t)$ as a time-dependent wave-vector. The pressure fluctuation is removed from consideration using the divergence-free property, which amounts to $\boldsymbol{k}\cdot\hat{\boldsymbol{u}} = 0$. The solution of this equation is obtained for arbitrary initial data using a Green's function, as

$$\hat{u}_i(\boldsymbol{k}(t), t) = G_{ij}(\boldsymbol{k}(t'), t, t')\hat{u}_j(\boldsymbol{k}(t'), t').$$

Time history of $\boldsymbol{k}$ is given by a linear relationship

$$k_i(t) = F^{-1}_{ji}(t, t')k_j(t'), \tag{9}$$

where F_{ij} is the Cauchy matrix of the basic flow, obtained from A_{ij} by exponentiation. The latter equation is very similar to the mean trajectory equation in physical space

$$x_i = F_{ij}(t, t')X_j, \tag{10}$$

where $\boldsymbol{X}$, sometime called 'Rogallo space', are the Lagrangian coordinates for the mean flow. In the same way, $\boldsymbol{k}(t')$ at a fixed time origin, could be called $\boldsymbol{K}$, and the equations could be developed with respect to 'Lagrangian' wavevectors only.

In the presence of an additional right-hand-side term $f_i(\boldsymbol{k}, t)$ in eq. (7), which represents nonlinearity (and possibly random forcing), the previous solution can be generalized as

$$\hat{u}_i(\boldsymbol{k}(t), t) = G_{ij}(\boldsymbol{k}(t'), t, t')\hat{u}_j(\boldsymbol{k}(t'), t') +$$

$$\int_{t'}^{t} G_{ij}(\boldsymbol{k}(t'), t, \tau)f_j(\boldsymbol{k}(\tau), \tau)d\tau. \tag{11}$$

The latter equation is generic, and similar forms can be found for the equations which govern the statistical moments of $\hat{\boldsymbol{u}}$ at any order. In a slightly different form, one can introduce a new variable $\boldsymbol{a}$ as

$$\hat{u}_i(\boldsymbol{k}(t), t) = G_{ij}(\boldsymbol{k}(0), t, 0)a_j(\boldsymbol{k}(0), t) \tag{12}$$

which replaces the initial data in the linear solution, and can be considered as *slowly* varying in time (the initial time is fixed at $t' = 0$). The idea in applying generalized EDQNM is to transfer the 'machinery' of EDQNM procedures/assumptions from the $\hat{\boldsymbol{u}}$ to the slow variables $\boldsymbol{a}$. A cartoon of the optimal procedure, called EDQNM3, can be given as follows:

- Quasi-Normal (QN) procedure is the same, working with $\hat{\boldsymbol{u}}$ or with $\boldsymbol{a}$ variables. Fourth-order correlations at three points are expressed in terms of products of second-order correlations.
- Markovian (M) procedure consists in freezing the time dependency of the slow variables, and of the slow variables only, in the time integral which links third-order to second order correlations, once the QN assumption used.
- Eddy-Damping consists of replacing the 'bare' RDT Green's function by a viscous, and possibly renormalized one as

  $$G^{+}_{ij}(\boldsymbol{k}, t, t') = G_{ij}(\boldsymbol{k}, t, t')V(\boldsymbol{k}, t, t'), \tag{13}$$

  V being specified later.

In addition to the renormalization of **G** by a scalar term, the problem of renormalizing the Cauchy matrix in (9) is touched upon in the last section, together with the two-time aspect in general. The procedure has to be discussed case by case, as shown in the following.

As far as possible, eigenmode decomposition will be used to diagonalize **G**. At least, a drastic reduction of the number of variables will be obtained in working with the components in the Craya-Herring frame or in similar frames of references. For instance, a reduced Green's function can be used in the Craya-Herring frame of reference, as

$$u^{(\alpha)}(\boldsymbol{k}(t), t) = g_{\alpha\beta}(\boldsymbol{k}, t, t')u^{(\beta)}(\boldsymbol{k}(t'), t') \quad (14)$$

as used in my Ph. D. (thèse d' état, 1982) and in all subsequent papers in my team, 'Greek' indices taking the value 1 or 2 only, with Einstein convention understood.

3.2 Recent progress in basic EDQNM for isotropic turbulence

Isotropic turbulence is characterized by $Z = e = 0$ in (3). Only $U(k)$ is relevant, or equivalently, the spherically averaged spectrum $E(k)$, with

$$U(k) = \frac{E(k)}{4\pi k^2}. \quad (15)$$

The relevant dynamical equation is the Lin equation

$$\frac{\partial E}{\partial t} + 2\nu k^2 E = T \quad (16)$$

The EDQNM, introduced by Orszag [10] in close connection with Kraichnan's earlier studies, offered a reliable way to close the transfer term $T(k,t)$. In this case, however, there are only heuristic arguments for justifying the 'machinery': **G** reducing to the identity, only $V(k,t,t')$ in (13) can be considered as a 'rapid' term, allowing a better relaxation of fourth order cumulants in terms of triple ones, so that an 'a posteriori Markovianization' is eventually justified. Choosing $V(k,t,t') \sim \exp[-\mu(k,t)(t-t')]$, the eddy damping (+ viscous laminar term νk^2) μ is an important parameter. The structure of the EDQNM closure is

$$T(k) = \int\int_{\Delta_k} \theta_{kpq} A_{kpq} U(q) \left(U(p) - U(q)\right) dpdq,$$

with $\theta_{kpq} = (\mu(k) + \mu(p) + \mu(q))^{-1}$ being the heuristic triadic time-scale, resulting from $\int_{-\infty}^{t} V(k,t,t')V(p,t,t')V(q,t,t')dt'$. The geometric factor A_{kpq} derives from products of projection operators, and therefore reflects the 'true' structure of incompressible Euler equations (in contrast with shell models). Some recent applications and improvements by Bos and Bertoglio deserve some comment. The classical model was applied in the purely inviscid case [15] with very high resolution in k, and compares well to DNS of truncated Euler equations [16]. As shown in Fig. 2, in addition to the 'thermalized' tail in k^2 (equipartition for $U(k)$) constructed for $E(k)$, and the inertial $k^{-5/3}$ slope, a significant sink appears between them. This sink reproduces a kind of conventional dissipative range —but at zero laminar viscosity—, probably mediated by the non-local viscosity (Kraichnan, Lesieur & Schertzer), and is even clearer in EDQNM than in DNS. A recent improvement, which renders EDQNM closer to a self-consistent theory, consists of evaluating the eddy damping $\mu(k,t)$ using an additional dynamical equation for a velocity-position cross correlation [17]. As shown in Fig. 3, a realistic value of the Kolmogorov constant is derived, without need to specify it a priori in the model for μ.

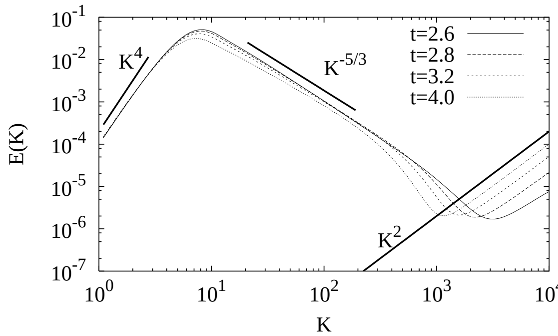

Fig. 2. The purely inviscid case using classical EDQNM

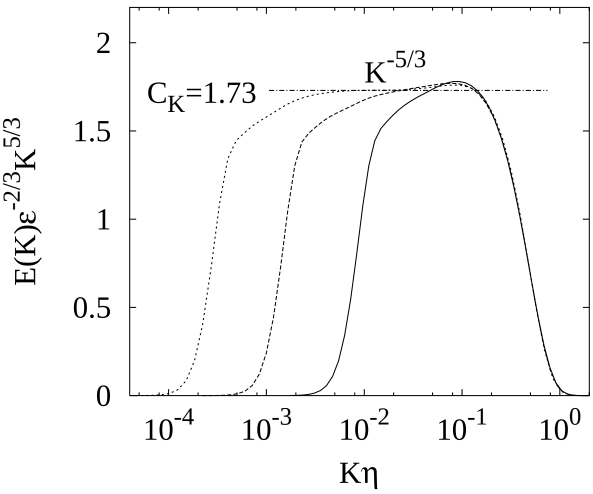

Fig. 3. Self-consistent eddy damping. Kolmogorov constant.

4 PURE ROTATION

This case corresponds to the general context of the previous section if an antisymmetric mean velocity gradient is chosen

$$A_{ij} = \epsilon_{inj}\Omega_n,$$

and the Cauchy matrix **F** reduces to an orthogonal matrix **Q**. Of course it is simpler to project both spatial coordinates and velocity vectors in the rotating frame, or

$$x_i \to Q_{ij}x_j, \quad u_i \to Q_{ij}u_j,$$

so that $\boldsymbol{u}, \boldsymbol{x}$ now represent variables seen in the rotating frame. We do not change the notation, however, for instance using $\boldsymbol{X}$ instead of $\boldsymbol{x}$ in agreement with (9), for the sake of simplicity. Consequently, the advection effect is removed from consideration, $\boldsymbol{k}$ (in fact $\boldsymbol{K}$ from (9)) is no longer time-dependent, and the effect of rotation is only reflected by additional body forces in the Navier-Stokes equations. Since the centrifugal force can be incorporated in the pressure gradient term, in the incompressible case, only the Coriolis force is present. The basic equation is

$$\frac{\partial u_i}{\partial t} + \underbrace{2\epsilon_{inj}\Omega_n u_j}_{\text{Coriolis}} + \frac{\partial p}{\partial x_i} = \nu\nabla^2 u_i - \underbrace{u_j\frac{\partial u_i}{\partial x_j}}_{\text{nonlinear}} .$$

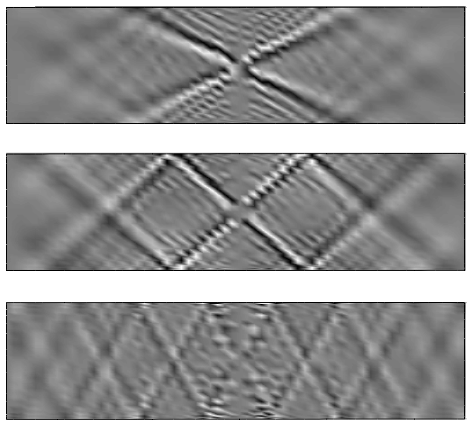

Fig. 4. Saint-Andrew cross shaped inertial waves emanating from a localized time-harmonic forcing. DNS by [18]

4.1 linear solution and 'slow' variables

To find the solution of the linearized inviscid equation, dropping out the right-hand-side in the latter equation, is not a trivial task: the Coriolis force is not divergence-free, so that the pressure fluctuation keeps its role to ensure incompressibility. Accordingly, the solution of the Cauchy problem is integro-differential in physical space, and the general method of the previous section is needed. In the general equation (11), the Green's function can be expressed as

$$G_{ij}(\boldsymbol{k}, t, t') = \Re\left(N_i(-\boldsymbol{k})N_j(\boldsymbol{k})e^{\imath\sigma_k(t-t')}\right) \quad (17)$$

and $\boldsymbol{k}$ $(= \boldsymbol{K})$ is constant. The unsteadiness of this solution depends on σ_k, which is nothing else than the unsigned dispersion frequency of inertial waves

$$\sigma_k = 2\boldsymbol{\Omega}\cdot\frac{\boldsymbol{k}}{k}. \tag{18}$$

More details on inertial waves can be found in Greenspan's monograph [19]. A typical 'Saint-Andrew cross' configuration is shown in Fig. 4, from DNS [18], reproducing experimental approaches by Mc Ewan and Mowbray & Rarity.

In a slightly different way, the linear solution yields

$$\hat{\boldsymbol{u}} = a_{+1} e^{\imath \sigma_k t} \boldsymbol{N} + a_{-1} e^{-\imath \sigma_k t} \boldsymbol{N}^* \tag{19}$$

In the linear limit, the $a_{\pm 1}$ are constants related to the initial data. In addition, these 'slow amplitudes' can be considered as a new set of time-dependent variables, and the equation above only reflects a bijective change of variables (sometime called 'Poincaré transform') from ($\hat{u}_i$, $i = 1, 2, 3$, $k_i \hat{u}_i = 0$) to $a_{\pm 1}$, *without any assumption*.

4.2 Wave-Turbulence, EDQNM3 and DNS

Continuing with the structure of equations without any assumption, the $a_s, s = \pm 1$ satisfy the following 'exact' equation:

$$\frac{\partial a_s}{\partial t} + \nu k^2 a_s =$$

$$\sum_{s', s'' = \pm 1} \int_{\boldsymbol{k}+\boldsymbol{p}+\boldsymbol{q}=0} e^{-\imath (s\sigma_k + s'\sigma_p + s''\sigma_q)t} \times$$

$$\times m_{ss's''}(\boldsymbol{k}, \boldsymbol{p}) a^*_{s'}(\boldsymbol{p}, t) a^*_{s''}(\boldsymbol{q}, t)\, d^3\boldsymbol{p} \tag{20}$$

in which the coupling term $m_{ss's''}$ derives from the basic Navier-Stokes equations in the helical decomposition [13,14]. Equation (20) demonstrates the importance of the resonant triads $\sigma_k \pm \sigma_p \pm \sigma_q = 0$ that appear when the phase term in (20) is zero :

$$\frac{k_\parallel}{k} \pm \frac{p_\parallel}{p} \pm \frac{q_\parallel}{q} = 0 \quad \text{with} \quad \boldsymbol{k} + \boldsymbol{p} + \boldsymbol{q} = \boldsymbol{0}. \tag{21}$$

Resonant and almost resonant triads are expected to dominate nonlinear slow motion, since significant non zero values of $k_\parallel/k \pm p_\parallel/p \pm q_\parallel/q$ in the r.h.s. of (20) severely damp the nonlinearity by scrambling. In that case, why not obtain a simplified model by solving equation (20) with an integral restricted to the resonant triads? Because the resonant surfaces are sufficiently complex to require very accurate interpolation, rendering the resulting computation relevant only for a smooth distribution of the slow amplitudes a_s in Fourier space. Such a smooth distribution cannot represent turbulence, so that one has to resort to describing statistical quantities instead, which are naturally smooth.

The transfer of the EDQNM machinery from $\hat{\boldsymbol{u}}$ to $a_{\pm 1}$ was used for this purpose, it is particularly simple in this case, for two reasons:

i) Because the helical modes generate the eigenmodes of the Curl operator, they not only simplify (diagonalize) the linear operator, they also simplify the basic quadratic nonlinear operator. In fact a relationship as (6,19) can render the nonlinear coupling simpler, as shown by Cambon (1982), Cambon & Jacquin [13], and Waleffe [14], even in the absence of rotation. This simplification ultimately comes from the form $\boldsymbol{u} \times \boldsymbol{\omega}$, up to gradient terms, of the basic nonlinearity.

ii) Only constant $\boldsymbol{k}$ are needed, so that the advection term by the solid body motion can be completely removed from consideration. This is not possible in the presence of a mean velocity gradient A_{ij} with nonzero symmetric part, as we will see in section 6.

Second-order correlations are entirely generated by the set e, Z, $\mathcal{H}$, or equivalently by $< a_s^* a_{s'} >$, $s = \pm 1, s' = \pm 1$. Without any assumption, second order correlations are governed by the following system of equations

$$\left(\frac{\partial}{\partial t} + 2\nu k^2\right) e = T^{(e)} \tag{22}$$

$$\left(\frac{\partial}{\partial t} + +2\imath\sigma_k + 2\nu k^2\right) Z = T^{(Z)} \tag{23}$$

$$\left(\frac{\partial}{\partial t} + 2\nu k^2\right) \mathcal{H} = T^{(h)} \tag{24}$$

It appears that the Coriolis force does not affect the (linear) left-hand-sides, except for the polarization parameter. Replacing Z by ζ, with

$$Z(\boldsymbol{k}, t) = e^{2\imath\sigma_k t}\zeta(\boldsymbol{k}, t), \tag{25}$$

and T^z by $e^{2\imath\sigma t}T^\zeta$, only the left-hand-side terms, which are linked to triple correlations and mediated by nonlinearity, are possibly rotation-dependent.

Ignoring provisionally $\mathcal{H}$ and ζ contributions, EDQNM3 (or equivalently EDQNM2 [13], the two versions differ only in treating Z) yields the following closure for the Lin equation:

$$T^{(e)} = \sum_{s', s''=\pm 1} \int\int\int \frac{A(k, s'p, s''q)}{\mu_{kpq} + \imath(\sigma_k + s'\sigma_p + s''\sigma_q)}$$

$$\times e(\boldsymbol{q})\left(e(\boldsymbol{p}) - e(\boldsymbol{k})\right) d^3\boldsymbol{p}. \tag{26}$$

The denominator reflects the time-integration of a product of three 'eddy damped' Green's functions, from eqs. (17) and (13).

In the limit of very high rotation rate, or at vanishing Rossby number, the asymptotic version of this equation is obtained using a Riemann-Lebesgue relationship for distributions

$$\frac{1}{\mu + \imath x} \to \pi\delta(x) + \mathcal{P}\left(\frac{1}{x}\right) \quad \text{when} \quad \mu \to 0$$

(sometime called Plemelj or Sokhotsky formula). Finally, the AQNM (A for asymptotic) theory is written

$$T^{(e)} = \sum_{s', s''=\pm 1} \int\int_{S_{s's''}} \pi \frac{A(k, s'p, s''q)}{s'\boldsymbol{C}_g(\boldsymbol{p}) - s''\boldsymbol{C}_g(\boldsymbol{q})}$$

$$\times e(\boldsymbol{q})\left(e(\boldsymbol{p}) - e(\boldsymbol{k})\right) d^2\boldsymbol{p} \tag{27}$$

in which $S_{s's''}$ is the resonant (family of) surface(s) and $\boldsymbol{C}_g(\boldsymbol{k})$ the group velocity of inertial waves. μ no longer appears in the final equation, whereas the denominator reflects that the reduction from a volume to a surface integral calls into play the gradient of resonant surfaces. The reader is referred to [23] for complete EDQNM3 equations (without $\mathcal{H}$) and to [21] for AQNM equations for e, ζ, $\mathcal{H}$.

4.3 Recapitulations of results

Starting from isotropic initial data, with a narrow-band energy spectrum, an inertial zone is constructed solving AQNM e-equation at vanishing Rossby number and infinite Reynolds number, until the inertial range reaches the maximum wavenumber. At this stage, laminar viscosity is reintroduced, and a self-similar shape is obtained. The spherically averaged energy spectrum $E(k)$ is constructed with a k^{-3} slope, as shown in Fig. 5, but the prefactor is $E(k) \sim \frac{\Omega}{t}k^{-3}$. Axisymmetric shape, with strong directional anisotropy, is found for the angle-dependent spectrum $4\pi k^2 e(k, \cos\theta, t)$, as shown on Fig. 6. This directional anisotropy, only mediated by nonlinear transfer, is consistent with the sketch on Fig. 7-c, and with all previous theoretical and numerical studies by [13,14,20], and therefore illustrates a transition from 3D (e equidistributed on spherical shells) to 2D structure (e concentrated on the horizontal waveplane). Nethertheless, the two-dimensionalization is limited to large k, and is never fully achieved. k^{-3} slope for E results from averaging various slopes for $4\pi k^2 e$, ranging from k^{-2} (quasi-horizontal wave-vectors) to k^{-5} (quasi-vertical wave-vectors). The relevance of this asymptotic result is perhaps marginal, since the time scale to reach the inertial zone constructed via weak wave-turbulence is very high, $\Omega\tau \sim O(R_o^{-2})$ at very small Rossby number R_o. In this context, it is interesting to note that a similar result was obtained by a high resolution (512^3) DNS, therefore at moderate R_o, Re and elapsed time, as shown on Fig. 8.

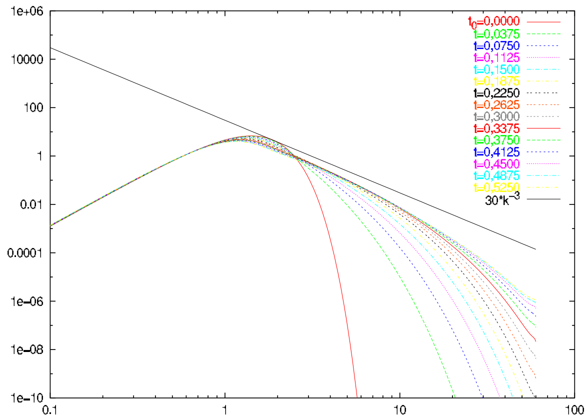

Fig. 5. Construction of the spherically averaged spectrum in AQNM [21]

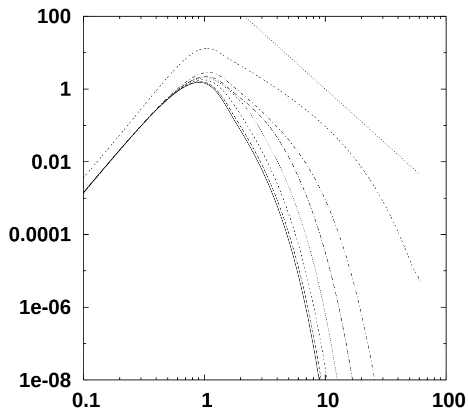

Fig. 6. Asymptotic angular dependent spectra from AQNM [21]

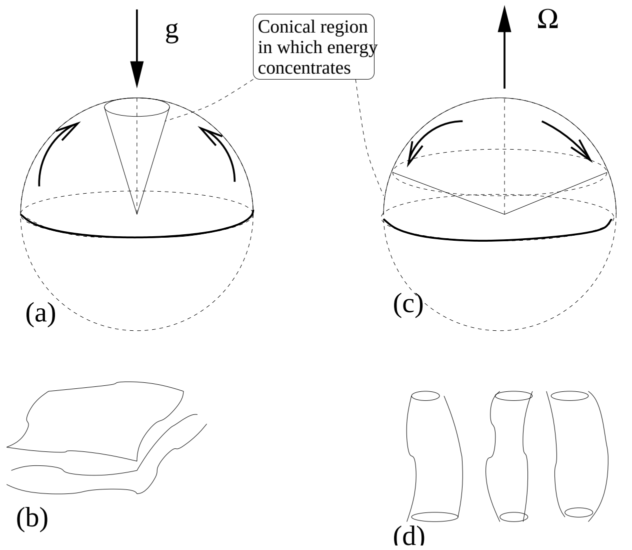

Fig. 7. Angular energy drain for (c) rotating and (a) stably stratified turbulence, spectral structure (a-c) versus shape in physical space (b-d).

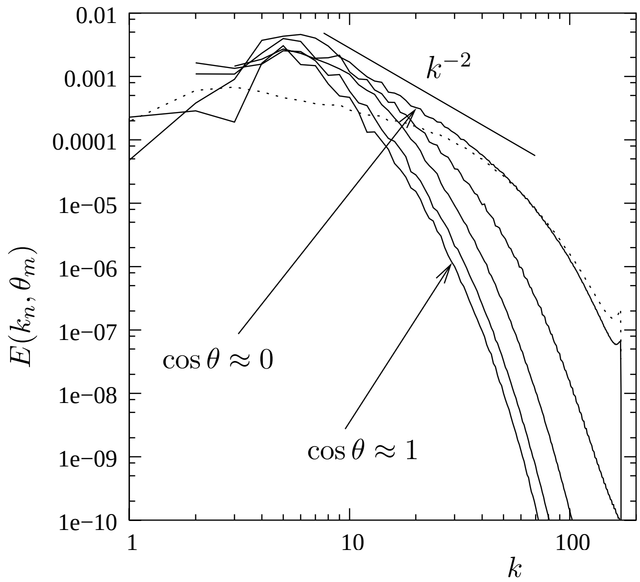

Fig. 8. Angular dependent spectra of purely rotating turbulence. A comparable isotropic spectrum of the same quantitiy is shown as a black dotted line. [30,34]

4.4 Open issues

These issues will be discussed in a more detailed way in the final version (to be included in a book).

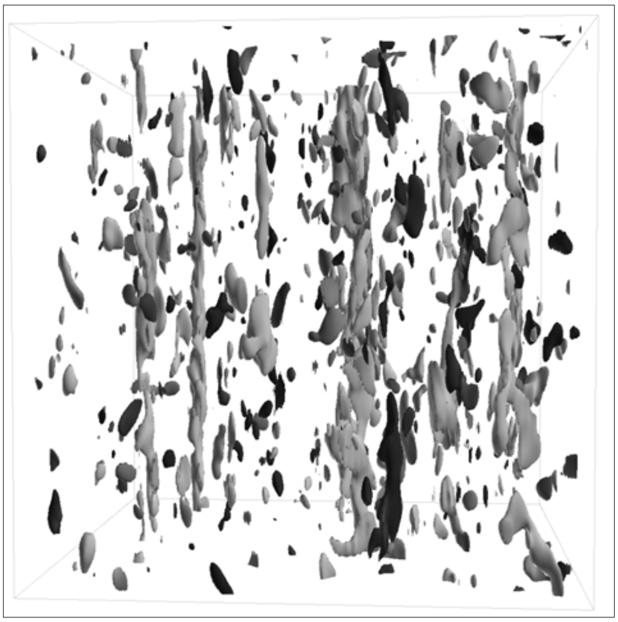

Fig. 9. Isovorticity surfaces from recent high resolution DNS. Dominantly cyclonic structures are in grey.

Five themes, interconnected each other, will be addressed :

i) Saturation of trends towards two-dimensionalization. Discussion of the discrete versus the continuous case, influence of solid boundaries and of Ekman pumping. Can the dissipative zone be really quasi-2D ?

ii) Treatment *per se* of the slow manifold in the continuous case, with relevant statistical quantities to measure and to compute [23,24].

iii) Asymmetry between cyclonic and anticyclonic vorticity at intermediate Rossby number. [25]. This theme is illustrated on Fig. 9 [30,34] and on Fig. 10. from [26]. Statistical theory will be revisited and confronted to arguments from stability analysis.

iv) What can be retained from under-resolved conventional DNS/LES ? Two-componentalization or two-dimensionalization ?

v) Subtle interplay between linear [28] and nonlinear mechanisms. Is pure linear theory relevant ? Discussion of the recent study by Davidson *et al.* [29].

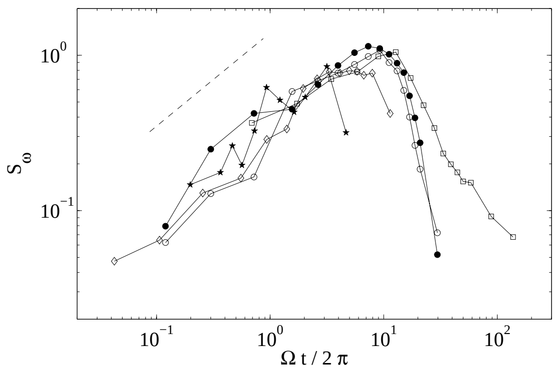

Fig. 10. Time history of the vertical vorticity skewness. A positive value quantifies the prevalence of cyclonic vorticity. Experimental results.

5 Stable stratification

The flow is now considered as subjected to a buoyancy force, which results from an imbalance between the weight of the particle and the ambient buoyancy. The buoyancy force $b\boldsymbol{n}$ is along the vertical unit vector denoted $\boldsymbol{n}$, with magnitude b. In addition, the fluid is stably density-stratified, with a constant vertical mean density gradient, resulting in a constant Brunt-Vaisala frequency N. The coupled equations for $\boldsymbol{u}$ and b in the Boussinesq approximation are

$$\frac{\partial \boldsymbol{u}}{\partial t} - \underbrace{b\boldsymbol{n}}_{\text{buoyancy}} + \frac{\partial p}{\partial x_i} = \nu\nabla^2 u_i - \underbrace{u_j\frac{\partial u_i}{\partial x_j}}_{\text{nonlinear}} \quad (28)$$

$$\frac{\partial b}{\partial t} + \underbrace{N^2\boldsymbol{u}\cdot\boldsymbol{n}}_{\text{stratification}} = \kappa\nabla^2 b - \underbrace{u_j\frac{\partial b}{\partial x_j}}_{\text{nonlinear}} \quad (29)$$

the velocity fluctuation *remaining solenoidal (divergence-free) although the density can fluctuate*. These equations are valid for a liquid (b would be related to the fluctuating density) or for a gas (b would be related to the temperature fluctuation) with the same form. Only the diffusion coefficient of the stratifying agent (salt, temperature), κ, distinguishes different physical flows.

5.1 linear inviscid solution, slow variables

Linear solutions are very similar to the ones in the rotating case. As before, the number of components in Fourier space is reduced, using the Craya-Herring frame, but the buoyancy must be accounted for. The buoyancy mode is chosen along the third component (Fig. 1), or

$$u^{(3)} = \imath \frac{\hat{b}}{N}, \tag{30}$$

similarly to a pseudo-dilatational velocity mode (a true dilatational velocity mode will be addressed in section 8). Equivalently, a new vector $\hat{\boldsymbol{v}}$ can be defined in the fixed frame of reference

$$\hat{\boldsymbol{v}} = \hat{\boldsymbol{u}} + \imath \frac{\hat{b}}{N},$$

with components $u^{(1)}$ (toroidal velocity), $u^{(2)}$ (poloidal velocity) and $u^{(3)}$ (buoyancy) in the Craya-Herring frame. The problem with five components (u_1, u_2, u_3, p, b) in physical space therefore reduces to a three-component problem $(u^{(i)}, i = 1, 2, 3)$ in Fourier, Craya-Herring, space. As previously, the linear solution yields

$$\hat{\boldsymbol{v}} = a_0 \boldsymbol{N}^{(0)} + a_{+1} e^{\imath \sigma_k t} \boldsymbol{N}^{(1)} + a_{-1} e^{-\imath \sigma_k t} \boldsymbol{N}^{(-1)} \tag{31}$$

with $a_s, s = 0, \pm 1$ constant in the linear limit, or else new time-dependent 'slow' variables in the general nonlinear case. The presence of a third mode, related to the slow amplitude a_0, is an essential difference with respect to the rotating case. This mode, involving the toroidal velocity and called a 'vortex' mode by Riley et al. [32], is not a degeneracy of the wave modes at vanishing dispersion frequency. σ_k in Eq. (31) is now the dispersion frequency of gravity waves

$$\sigma_k = N \frac{|\ \boldsymbol{k} \times \boldsymbol{n}\ |}{k}. \tag{32}$$

Accordingly, a slow 'singular' wave-mode exists, but only for vertical wave vectors.

As a final problem dealing with linear solutions, we discuss the role of laminar diffusion. If $\kappa = \nu$ (Prandtl or Schmidt number equal to 1), the linear solution is only modified by a scalar damping factor. If not, the nature of the solution can be altered, in connection with the sign of a discriminant

$$\Delta = \left((\kappa - \nu)^2 k^2\right)^2 - (2\sigma_k)^2.$$

The wave regime (temporal oscillations in Fourier space) persists only if $\Delta < 0$, but disappers if $\Delta > 0$ and is replaced by viscous damping only. *This result is generic of wave regimes with two different diffusivities*, as we will also see in sections 7 and 8.

5.2 Nonlinear statistical equations

Very similarly to the rotating flow case, the statistical equations [31] are

$$\left(\frac{\partial}{\partial t} + 2\nu k^2\right) e^{(tor)} = T^{(tor)} \tag{33}$$

$$\left(\frac{\partial}{\partial t} + 2\nu k^2\right) e^{(pol+pot)} = T^{(pol+pot)} \tag{34}$$

$$\left(\frac{\partial}{\partial t} + +2\imath\sigma_k + 2\nu k^2\right) Z' = T^{(Z')} \tag{35}$$

(assuming $\kappa = \nu$), but two kind of energy are conserved, the toroidal energy and the total wave energy, the sum of poloidal and potential energies. An oscillating variable, denoted Z', characterizes the lack of equipartition between poloidal and potential energy. A last quantity, linked to the imaginary poloidal buoyancy flux, is similar to the helicity in the rotating flow case and is ignored for the same reason.

5.3 Results, EDQNM2, DNS, and discussion

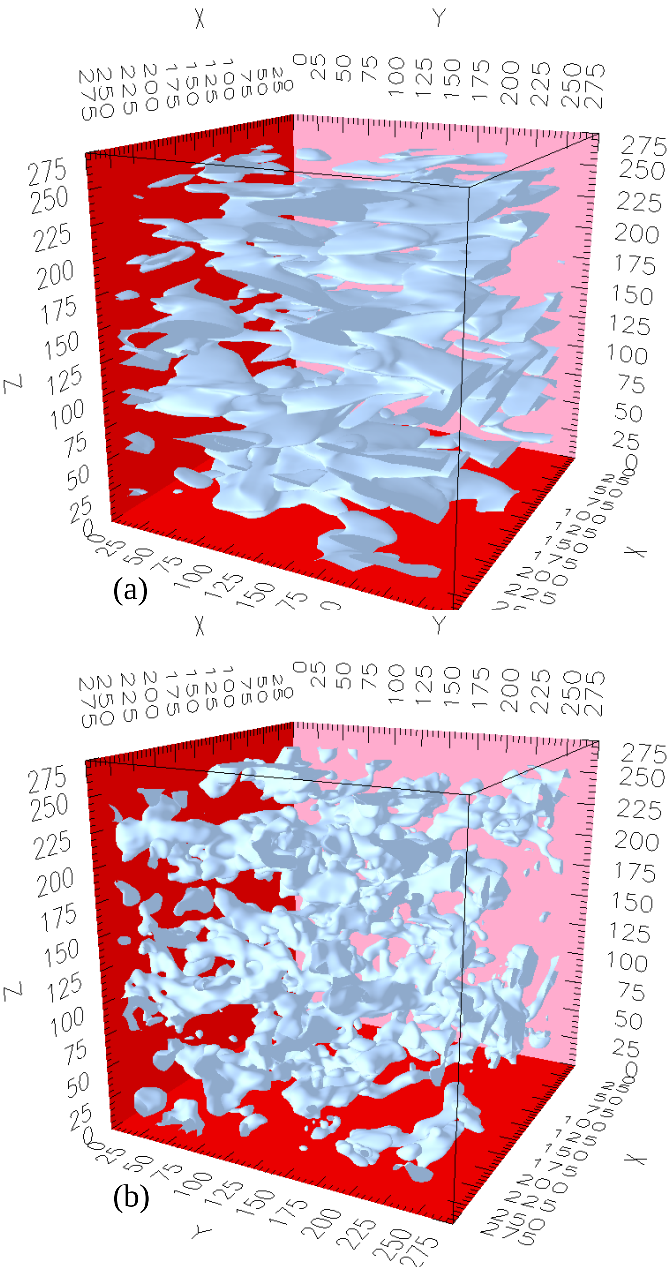

Fig. 11. Iso-velocity surfaces of purely stratified turbulence, from DNS [34]. The velocity field has been decomposed in the (a) toroidal and (b) poloidal parts. One observes the large anisotropy in the toroidal part and the relative isotropy in the poloidal part of the velocity field.

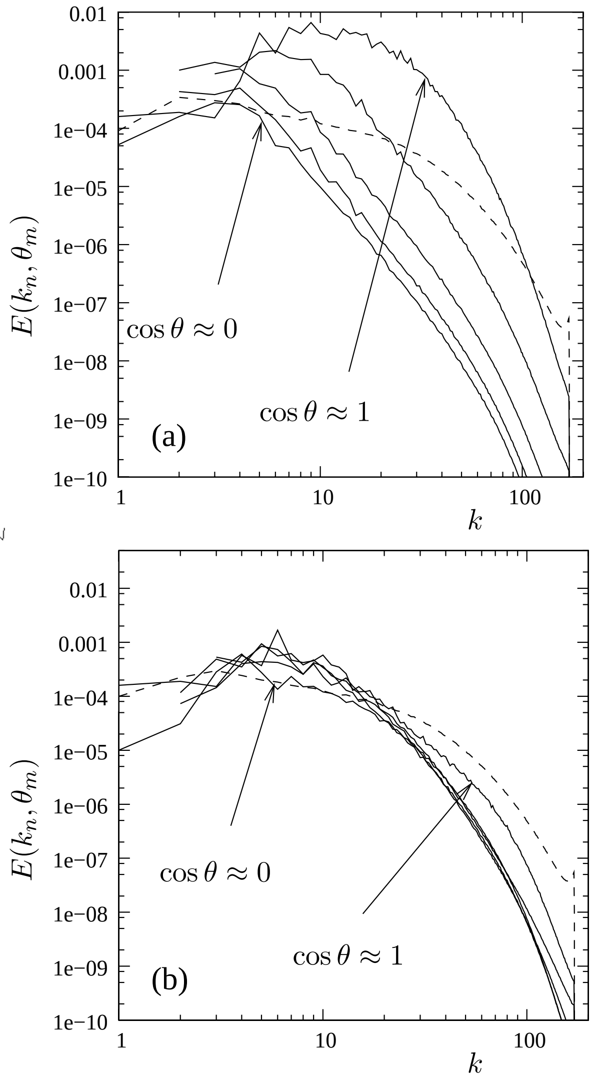

Fig. 12. Angular dependent spectra of purely stratified turbulence, from 512^3 DNS [30,34]. The spectral energy has been decomposed into its (a) toroidal and (b) poloidal contribution. A comparable isotropic spectrum of the same quantitiy is shown as a black dotted line.

EDQNM2 [31] was used to close eq. (33-35). The results suggested that the horizontal layering (sketched on Fig. 7-b) is essentially due to an angular energy drain towards vertical wave-vectors (Fig. 7-a). In addition, this effect mainly affected the toroidal (or vertical vortex) mode. Even if EDQNM2 is not so satisfactory than EDQNM3, overestimating the oscillating mode Z' in Eq. (35), it compared very well with DNS results, even looking at the finest statistical quantities [33]. Very recently, high resolution DNS have confirmed all these features. As shown on Fig. 11, the contribution of the toroidal mode to the layering is dominant. This is quantified in spectral space using angle-dependent spectra for both toroidal and poloidal modes. The poloidal component, affected by gravity waves, exhibits a clear k^{-2} law in DNS [30], with a quasi-isotropic angular distribution. In this sense, the behaviour of strongly stratified flow is not quasi-2D but anti-2D (comparing sketchs 7-a and 7-c). This fact is not recognized with sufficient clarity, perhaps because of the confusion between 'horizontal', '2D' and 'toroidal', usual in the geophysical community —influenced by shallow waters models ? — . On the one hand, our approach is consistent with the one by Billand & Chomaz [35] and by Lindborg [36], who stressed that the dynamics of stably stratified turbulence has nothing to do with 2D dynamics. On the other hand, our angle of attack is essentially statistical, allowing anisotropic structuring, but without initially large coherent vertical vortices, as needed for triggering a zig-zag instability [35]; in the same way, we prefer avoid geometric constraints, such as strongly flattened boxes in DNS, and quasi-2D forcing, used by [36]. All the results encourage us to continue to develop statistical models, EDQNM3 type, towards parameter ranges far outside the domain of DNS. The concept of 'toroidal turbulence' could reconcile the different approaches to strongly stratified turbulence.

The formalism is readily generalized, combining rotation, with Coriolis parameter f (instead of 2Ω) and stable stratification for an arbitrary range of f/N ratios. Linear solutions are easily found, with eigenmodes in the Craya-herring frame (e.g. [50]), and nonlinear statistical equations, similar to (33-35) are found in terms of them, replacing the toroidal mode (a_0-type amplitude with $e^{(tor)}$ energy) by a quasi-geostrophic (QG) mode , and the gravity-wave modes ($a_{\pm 1}$-type amplitudes) by the inertia-gravity wave-modes. At least for f/N not too large, a quasi-geostrophic model can be derived, as a natural extension of 'toroidal turbulence'. On the one hand, it is important to point out that our QG mode corresponds only to linearized potential vorticity, so that the quasi-geostrophic counterpart of equations (33-35) cannot be directly compared to the more general (nonlinear) formulation by Charney [37] and many others. On the other hand, the linear eigenmodes are unexpectedly relevant for analyzing nonlinear couplings. Finally, a quasi-geostrophic model based on EDQNM-type closure was already proposed by Herring [38], but with an additional assumption of very weak anisotropy; relaxing this assumption offers new perspectives for EDQNM3, for a large range of f/N ratios.

6 Issues for pure shear

The general case of constant **A**, adressed in my Ph. D. thesis and in [2] is not rediscussed here for the sake of brevity. In addition to pure straining processes related to irrotational mean flows (**A** symmetric), two-dimensional mean flows are characterized by elliptical, linear or hyperbolic streamlines. Linear solutions allows exponential growth in both elliptical and hyperbolic case, and only algebraic growth in the 'linear' case. Since exponential growth induces issues in nonlinear closure theories, which are not completely mastered, only the later case, or pure plane shear, is addressed in this section.

Mean shear flows are ubiquitous in turbulence. In a real flow, the shear is allways created by the wall, except in the absence of mean velocity parallel to the fixed wall or when the wall is a belt moving with the same velocity as the flow. Shear flow is therefore intimately connected with near wall turbulence dynamics. Nevertheless, many features can be understood in the idealized case of an uniform mean shear in the ab-

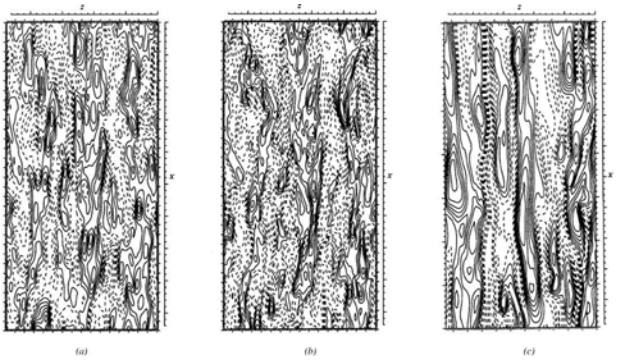

Fig. 13. Contours of streamwise fluctuating velocity in a horizontal plane from: (left) direct numerical simulation (nonlinear) of HAT at constant shear rate, (middle) purely linear calculations , and (c) direct numerical simulation of plane channel flow near a wall (horizontal plane $y^+ \sim 10$). The streamwise elongation of turbulent structures resulting from shear appears clearly, as does the strong similarity between RDT and DNS results. From Lee, Kim and Moin [40]

sence of boundaries, in the context of HAT (Homogeneous Anisotropic Turbulence). The relevance of this idealized model flow was discussed by W. C. Reynolds, among many others, as follows: the effect of the wall is to create a mean shear and to block the vertical motion; the uniform shear, a priori imposed, is also responsible for a reduction of vertical velocity fluctuation, so the presence of the wall is not so important than expected. In addition to statistical descriptors, even particular flow realisations can illustrate the relevance of linear dynamics, as shown on Fig. 13.

The mean flow is characterized by the following space-uniform mean velocity gradient matrix and Cauchy (or displacement gradient) matrix

$$A_{ij} = S\delta_{i1}\delta_{j2}, \quad F_{ij}(t) = \delta_{ij} + St\delta_{i1}\delta_{j2}, \qquad (36)$$

and components $1, 2, 3$ classically will be referred to as streamwise, cross-gradient (or vertical) and spanwise directions, respectively.

6.1 Linear solutions

Using the general formalism in (), RDT equations are

$$\dot{\hat{u}}_i + S\left(\delta_{i1} - 2\frac{k_1 k_i}{k^2}\right)\hat{u}_2 \qquad (37)$$

and

$$\dot{k}_i + Sk_1\delta_{i2} = 0. \qquad (38)$$

The latter equation generates the characteristic lines in Fourier space

$$k_1 = K_1, \quad k_2 = K_2 - StK_1, \quad k_3 = K_3 \qquad (39)$$

which are exactly related to the mean trajectories in physical space

$$x_1 = X_1 + X_2 St, \quad x_2 = X_2, \quad x_3 = X_3. \qquad (40)$$

(the latter two equations are a special case of $k_i = F^{-1}_{ji} K_j$ and $x_i = F_{ij} X_j$ using Eq. (36).) Taking advantage of the decoupling of the equation for $\hat{u}_2$, or

$$\dot{\hat{u}}_2 - 2S\frac{k_1 k_2}{k^2}\hat{u}_2 = 0,$$

and using $\dot{k}_i k_i = \dot{k}k = -Sk_1k_2$ from eq. (38), is found

$$(k^2 \dot{\hat{u}_2}) = 0,$$

which express that the Laplacian of the vertical velocity component is purely advected. Its solution is found as

$$\hat{u}_2(\boldsymbol{k}, t) = \frac{K^2}{k^2}\hat{u}_2(\boldsymbol{K}, 0). \qquad (41)$$

Finally, the complete solution are found as (e.g. Townsend [8], Piquet's book)

$$\begin{bmatrix} \hat{u}_1(\boldsymbol{k},t) \\ \hat{u}_2(\boldsymbol{k},t) \\ \hat{u}_3(\boldsymbol{k},t) \end{bmatrix} = \begin{bmatrix} 1 & G_{12} & 0 \\ 0 & \frac{K^2}{k^2} & 0 \\ 0 & G_{32} & 1 \end{bmatrix} \begin{bmatrix} \hat{u}_1(\boldsymbol{K},0) \\ \hat{u}_2(\boldsymbol{K},0) \\ \hat{u}_3(\boldsymbol{K},0) \end{bmatrix} \tag{42}$$

with two non-diagonal terms

$$G_{12} = -S\int\left(1-2\frac{K_1^2}{k^2}\right)\frac{K^2}{k^2}dt$$

and

$$G_{32} = 2S\frac{K_1K_3}{K^2}\int\frac{K^4}{k^4}dt,$$

in which the time dependency is induced by $k^2(t)$ from Eq. (39). Analytical integration is not difficult but rather teduous, and therefore not given here. Only for $K_1=0$, the solution is drastically simplified with $K/k=1$, $G_{12}=-St$, $G_{32}=0$.

This solution can be found with the minimum number of components in the Craya-Herring frame of reference. In contrast with axisymmetric flow cases, the choice of the polar axis $\boldsymbol{n}$ is not completely obvious, but an optimal choice does exist: choosing $\boldsymbol{n}$ in the vertical direction, $u^{(1)}$ and $u^{(2)}$ are connected to vertical vorticity and Laplacian of vertical velocity, respectively, and therefore are the spectral normalized counterparts of Orr-Sommerfeld-Squire variables. The system of two equations is

$$\dot{u}^{(\alpha)} + Se_1^{(\alpha)}e_2^{(\beta)}u^{(\beta)} = 0$$

since the terms $\dot{e}_i^{(\alpha)}e_i^{(\beta)}$ identically vanish. As for the solution in the fixed frame of reference, the (poloidal) $u^{(2)}$-equation

$$\dot{u}^{(2)} - S\frac{k_1k_2}{k^2}u^{(2)} = 0 \tag{43}$$

is decoupled. The toroidal equation reduces to

$$\dot{u}^{(1)} + S\frac{K_3}{k}u^{(2)} = 0 \tag{44}$$

so that the complete solution is

$$\begin{bmatrix} u^{(1)}(\boldsymbol{k},t) \\ u^{(2)}(\boldsymbol{k},t) \end{bmatrix} = \begin{bmatrix} 1 & g_{12} \\ 0 & \frac{K}{k} \end{bmatrix} \begin{bmatrix} u^{(1)}(\boldsymbol{K},0) \\ u^{(2)}(\boldsymbol{K},0) \end{bmatrix}, \tag{45}$$

in which the unique non-diagonal term is

$$g_{12} == \frac{KK_3}{K_1K_\perp}\left(\tan^{-1}\frac{k_2}{K_\perp} - \tan^{-1}\frac{K_2}{K_\perp}\right)$$

with $K_\perp = \sqrt{K_1^2+K_3^2}$, so that a complete solution is generated, much simpler than the one in the fixed frame of reference. As before, the particular case $K_1=0$ yields $K/k=1$ and $g_{12}=-St\frac{k_3}{k}$.

6.2 Issues for nonlinear statistical theories

The time-dependent wave-vector is an unavoidable aspect. Even using 'mean Lagrangian' wave-vector $\boldsymbol{K}$ (and similarly $\boldsymbol{P}$, $\boldsymbol{Q}$ for triads), k^2 remains time dependent, and related projection operators (or similarly $\boldsymbol{e}^{(\alpha)}$ or $\boldsymbol{N}$ vectors) become time-dependent in a non-trivial way (in contrast with rotating turbulence).

These difficulties appear even for pure linear inviscid, RDT, calculations, for instance for calculating the growth rate of kinetic energy as

$$\frac{q^2(t)}{q^2(0)} = \int\int_{|\boldsymbol{K}|=1} g_{\alpha\beta}(\boldsymbol{K},t,0)g_{\alpha\beta}(\boldsymbol{K},0)d^2\boldsymbol{K}.$$

In spite of the simplicity of the latter integral, and of the fact that $g_{\alpha\beta}$ is analytically expressed from Eq. (45), the final derivation of the kinetic energy history is not an easy task. The problem comes from the existence of two different solutions, the one for $K_1 = 0$ and the one for $K_1 \neq 0$, even if continuity holds. An expansion for high values of St yields a result which is not uniformly valid over the angular domain in $\boldsymbol{k}$: a substantial contribution to the integral comes from a narrow region of thickness $O[(St)^{-1}]$ near $K_1 = 0$ as St increases. This difficulty yielded Rogers (1991) to use matched asymptotic developments to derive the large St time-development of the turbulent kinetic energy, only the final result is given here for the sake of brevity: the growth rate is linear $q^2(St)/q^2(0) \sim St$. Even the case of viscous RDT is not completely analytically solved (Beronov and Kaneda, private).

One of the main challenge is to reproduce by statistical theory the transition from linear (algebraic) growth to nonlinear exponential growth. As a surprizing result, even if conventional single-point modelling methods cannot reproduce RDT, because of a flaw in the conventional closure of 'rapid' pressure-strain rate correlations, they apparently can predict nonlinear exponential growth of kinetic energy. This 'correct' behaviour only reflects the fact that all relevant non-dimensional ratios, from b_{ij} (the non-dimensional deviatoric part of the Reynolds stress tensor) to $\frac{q^2/2}{\varepsilon}$, can reach constant asymptotic values at large St, with a 'reasonable' level controlled by the tuned constants of the model. Consequently, the typical energy growth rate

$$\Lambda = \frac{1}{Sq^2}\frac{dq^2}{dt} \tag{46}$$

also reaches a constant value, in agreement with exponential growth for q^2.

Nevertheless, single-point modelling predict something but cannot reproduce RDT (e.g. streaklike structuring quantified by various integral lengthscales) and cannot explain its transition to nonlinear regime at different scale. More effort on two-point modelling is required for this purpose. Accordingly, detailled equations from DIA, LRA and EDQNM3 are being written in terms of $u^{(1)}, u^{(2)}$ variables, or in terms of the a_α ($a_1(\boldsymbol{K}, t)$, $a_2(\boldsymbol{K}, t)$) which must replace (EDQNM3) the initial variables ($u^{(\alpha)}(\boldsymbol{K}, 0)$) in Eq. (45).

7 Towards MHD flows

Simplified MHD flows are considered in the presence of a given, strong external magnetic fluid $\boldsymbol{B}$, in order to illustrate isotropy breaking (axisymmetric MHD turbulence).

7.1 linear solutions

In Fourier space, fluctuation of velocity, $\hat{\boldsymbol{u}}$, and fluctuation of the magnetic field, $\hat{\boldsymbol{b}}$, are governed by

$$\frac{\partial \hat{\boldsymbol{u}}}{\partial t} - \imath\lambda(\boldsymbol{B}\cdot\boldsymbol{k})\hat{\boldsymbol{b}} = 0 \tag{47}$$

$$\frac{\partial \hat{\boldsymbol{b}}}{\partial t} - \imath(\boldsymbol{B}\cdot\boldsymbol{k})\hat{\boldsymbol{u}} + \nu_m k^2 \hat{\boldsymbol{b}}, \tag{48}$$

with λ only related to susceptibility and density, ν_m being the magnetic diffusivity (Elsasser 1950, Moffatt [41], Alboussière [42]) . Laminar viscosity is neglected, and two nondimensional numbers are relevant: the magnetic Reynolds number R_m and the Lundquist number S_m .

Neglecting the magnetic diffusivity, Elsasser variables $\boldsymbol{u} \pm \lambda^{1/2}\boldsymbol{b}$ generate the relevant modes of Alfven waves, with the dispersion frequency

$$\sigma_k = \lambda^{1/2}\boldsymbol{B}\cdot\boldsymbol{k} = \boldsymbol{V}_m\cdot\boldsymbol{k}, \tag{49}$$

in which $\boldsymbol{V}_m$ is an equivalent magnetic velocity, describing pure planar non-dispersive waves. In spite of analogies with the stratified flow case, double diffusivity (here $\boldsymbol{b}$ diffuses but $\boldsymbol{u}$ does not) may have an important impact on the linear solution. The problem of interaction of waves with a double diffusivity aspect cannot be ignored.

In the general case, the solution of Eq. (47,48) displays the exponential rate

$$\beta_k = \nu_m \frac{k^2}{2}\left(1 \pm \sqrt{1-r^2}\right) \tag{50}$$

The crucial ratio r is

$$r = \frac{2\sigma_k}{\nu_m k^2}, \tag{51}$$

in agreement with the 'dumbell' diagram on Fig. 14. If $\mid r \mid \gg 1$ (inside the double sphere in Fig. 14), one recover the regime of Alfven waves, with an additional damping corresponding to $\Re(\beta) \sim -\nu_m \frac{k^2}{2}$. If $1 \gg \mid r \mid$ (far outside the double sphere), $\beta \sim \frac{\sigma_k^2}{\nu_m k^2} = \frac{V_m^2}{\nu_m}\cos^2\theta$ and the flow is essentially subjected to an anisotropic (directional dependence only !) Joule dissipation effect.

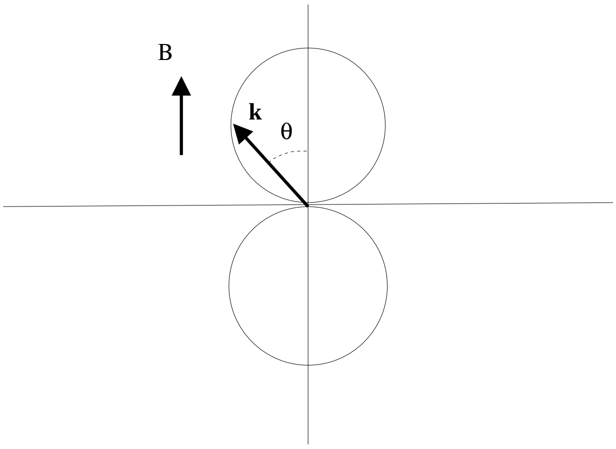

Fig. 14. The 'dumbell' picture. Spheres are given by equation $\frac{k}{\cos\theta} = \pm D$, with diameter $D = 2\frac{V_m}{\nu_m}$.

7.2 Wave-Turbulence and EDQNM3

Two régimes are well documented. On the one hand, the weakly nonlinear quasi-static case, with $1 \gg R_m$, $1 \gg S_m$, is dominated by Alfven waves, and Wave-Turbulence theory recently gave interesting results [43], even if the basic waves are not dispersive. On the other hand, the nonlinear case with $1 \gg R_m$, $S_m \gg 1$, is essentially Navier-Stokes turbulence subjected to an additional diffusive effect, or

$$\frac{V_m^2}{\mu_m}\cos^2\theta \boldsymbol{u}$$

to add in the left-hand side of Navier Stokes equations (in 3D Fourier space). EDQNM3 is being applied to these two cases and to intermediate régimes.

8 Towards weakly compressible, quasi- isentropic, flows

A true dilatational part of the flow can be reindroduced in the study, considering all three components in the Craya-Herring frame (Fig. 1)

$$\hat{\boldsymbol{u}} = \underbrace{u^{(1)}\boldsymbol{e}^{(1)} + u^{(2)}\boldsymbol{e}^{(2)}}_{\hat{\boldsymbol{u}}^s} + \underbrace{u^{(3)}\frac{\boldsymbol{k}}{k}}_{\hat{\boldsymbol{u}}^{(d)}}, \tag{52}$$

in agreement with the Helmholtz decomposition in physical space, the superscripts 's' and 'd' denoting solenoidal and dilatational modes, respectively. Compressible isentropic equations are

$$\dot{\rho} + \rho u_{i,i} = 0$$

$$\rho \dot{u}_i = -p_{,i}$$

$$\frac{\dot{p}}{p} - \gamma\frac{\dot{\rho}}{\rho} = 0$$

in which the 'overdot' denotes a full substantial derivative. Some additional simplifications are found if we consider that the fluctuations are weak with respect to a 'mean' state, with constant P and ρ_0, and no mean velocity. One can assume

$$p = c_0^2\rho, \quad c_0^2 = \gamma\frac{P}{\rho_0},$$

c_0 being the sonic speed, and consider the system with only two equations

$$\frac{\partial u_i}{\partial t} + \frac{1}{\rho_0}\frac{\partial p}{\partial x_i} = -u_j\frac{\partial u_i}{\partial x_j} \qquad (53)$$

$$\frac{\partial p}{\partial t} + \gamma P\frac{\partial u_i}{\partial x_i} = 0 \qquad (54)$$

These equations are the starting point for both the nonlinear (statistically isotropic) approach by Bertoglio and coworkers, and the RDT study by Simone et al. [44], revisited in subsection 8.2 and 8.3, respectively.

8.1 linear solutions

Dropping the right-hand-sides in the previous equations (53, 54), and using Fourier space, with Eq. (53) projected along $\boldsymbol{k}/k$, is found

$$\frac{\partial u^{(3)}}{\partial t} + \frac{1}{\rho_0}\imath k\hat{p} = 0$$

$$\frac{\partial \hat{p}}{\partial t} + \imath\gamma Pku^{(3)} = 0$$

Solutions involve $e^{\pm\imath kc_0t}$ terms, which correspond to the acoustic mode — or at least to the pseudo-sound —, with the dispersion frequency

$$\sigma_k = kc_0.$$

Of course, the solenoidal part of the flow, for instance generated by $u^{(1)}, u^{(2)}$ in the Craya-Herring frame, is conserved in the linear limit and gives the slow mode. Rescaling $\hat{p}$ as in Simone et al.[44], or

$$u^{(4)} = \imath\frac{\hat{p}}{\rho_0c_0}, \qquad (55)$$

$u^{(3)} \pm \imath u^{(4)}$ generate the slow wavy amplitudes $a_{\pm1}$, or

$$\left(u^{(3)} \pm \imath u^{(4)}\right)_t = e^{\pm c_0kt}\left(u^{(3)} \pm \imath u^{(4)}\right)_{t=0}. \qquad (56)$$

Reintroducing laminar diffusivity, we are faced again with a problem of double difusivity, since the pressure does not diffuse, whereas the dilatational velocity mode is affected by the coefficient $(4/3)\nu$. Accordingly, a discriminant is displayed as

$$\Delta = \left(\frac{4}{3}\nu k^2\right)^2 - (2c_0k)^2.$$

8.2 Nonlinear statistics

As for the case of buoyant turbulence in a stratified fluid, the basic equations in terms of 'slow' amplitudes are

$$\frac{\partial a_s}{\partial t} = \sum_{s',s''=0,\pm1}\int_{\boldsymbol{k}+\boldsymbol{p}+\boldsymbol{q}=0} \exp\left(-\imath\left(s\sigma_k + s'\sigma_p + s''\sigma_q\right)t\right) \times$$

$$\times m_{ss's''}(\boldsymbol{k},\boldsymbol{p})a^*_{s'}(\boldsymbol{p},t)a^*_{s''}(\boldsymbol{q},t)\,d^3\boldsymbol{p} \qquad (57)$$

Diffusive terms can be neglected for a preliminar discussion of couplings. Of course, the coupling coefficients $m_{ss's''}$ completely differ in the weakly compressible flow case from their counterparts in the solenoidal buoyant case subjected to stable stratification, and a_0 is two-component (solenoidal mode) in the first case. A similar cartoon, however, can be discussed in both flow cases, depending on the signs (s, s', s''), or triad polarities, as follows:

i) Non-propagating slow mode, $s = 0$. It is clear that the nonlinear dynamics will dominantly involve interactions between slow modes only, so that the leading terms may correspond to $s' = s'' = 0$: one recovers the 'toroidal turbulence' for the stratified flow case and pure incompressible dynamics for the weakly compressible flow case. The main difference is that incompressible isotropic turbulence is well understood, at least regarding energy spectrum and energy transfer, whereas toroidal turbulence is still under investigation. Consequently, a large Reynolds number

Kolmogorov energy spectrum can be specified and fixed for the solenoidal mode, as in Fig. 15.

ii) Our main interest in this subsection is for the mode related to $s = \pm 1$, generating 'dilatational velocity' and 'pressure' contributions, which are closely connected together or not via a possible acoustic equilibrium. It is very difficult to rank a priori the three kinds of interactions $(\pm 1, 0, 0)$, $(\pm 1, \pm 1, 0)$ and $(\pm 1, \pm 1, \pm 1)$ for (s, s', s''). The first one is never resonant, but cannot be completely removed from consideration if the order of magnitude of a_0 is much larger than the one of $a_{\pm 1}$. The second one will select resonant 'dyads', like $k \pm p = 0$. Only the third one will select resonant triads, as $k \pm p \pm q = 0$.

It is clear that Wave-Turbulence is only a part of the whole story, even irrelevant in some case (as the toroidal turbulence in the stably stratified case). A simplified EDQNM3 closure strategy is in progress for further investigations. In addition, it will help explaining former interesting results by Fauchet *et al.* [45], using a combination of EDQNM, DIA and DNS approach. This aproach is illustrated on Fig. 15.

8.3 Towards compressible shear flow

It is possible to linearize Eq. (53) around a mean flow with space uniform gradient **A**, together with the complementary pressure equation (54). A general case was addressed by [44], including mean compression/dilatation $A_{ii} \neq 0$, resulting in a possible volumetric ratio $J(t)$ and time-depending sonic speed $c(t)$.

In addition to irrotational strain, the effects of the pure plane shear were extensively analysed. RDT solutions are expressed in terms of $u^{(i)}, i = 1, 4$

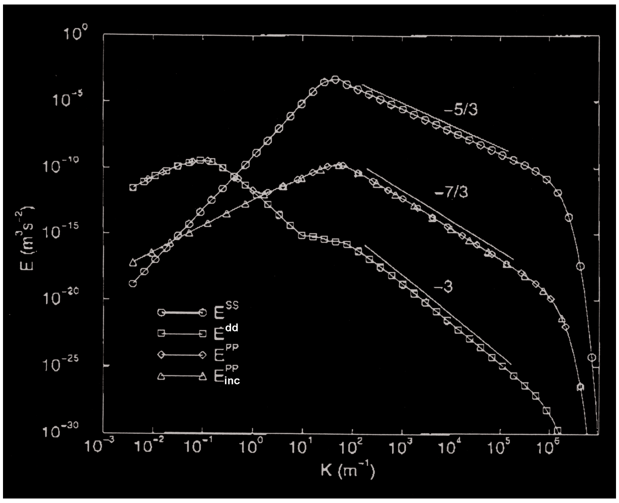

Fig. 15. Sketch of the spectra obtained by the model [45]. From top to bottom, at larger wavenumber, the figure shows the solenoidal (given) energy spectrum E^{ss}, the pressure variance spectrum E^{pp}_{inc} derived in the incompressible case, the pressure variance spectrum E^{pp}, and the dilatational energy spectrum E^{dd}. E^{pp} collapses with E^{dd} (acoustic equilibrium) only at smaller wavenumbers, whereas it collapses with E^{pp}_{inc} at larger wavenumbers, with $E^{pp} \gg E^{dd}$.

components, solving a linear system of ODE as:

$$\begin{pmatrix} \dot{u}^{(1)} \\ \dot{u}^{(2)} \\ \dot{u}^{(3)} \\ \dot{u}^{(4)} \end{pmatrix} = \begin{pmatrix} 0 & S\frac{K_3}{k} & m_{13} & 0 \\ 0 & -\frac{\dot{k}}{k} & m_{23} & 0 \\ m_{31} & m_{32} & m_{33} & -ck \\ 0 & 0 & ck & \frac{3-\gamma}{2}A_{ii} \end{pmatrix} \begin{pmatrix} u^{(1)} \\ u^{(2)} \\ u^{(3)} \\ u^{(4)} \end{pmatrix}$$

For instance, the 'solenoidal block', $m_{\alpha\beta}, \alpha = 1, 2, \beta = 1, 2$ is given above in the case of pure plane shear, in complete agreement with Eq. (43,44) in the incompressible RDT shear case. As in the incompressible case, Greek indices hold for the solenoidal space, with values $1, 2$ only, but new coupling terms are called into play, discussed below. Of course, the problem in four components in physical space (u_1, u_2, u_3, p) remains a four-components problem in Fourier, Craya-Herring space, no reduction of the number of variables is found as in all other solenoidal cases considered here, but at least, the matrix $m_{ij}, i = 1, 4, j = 1, 4$ has some zero components and the role of each nonzero component is clearer. The matrix depends on S ($\mathbf{A}$ in general) and on the dispersion frequency ck, hence it readily involves the spectral counterpart $\frac{S}{kc}$ of the 'distortion Mach number' [44] or 'gradient Mach number' [48], denoted M_d in Fig. 16 and 17.. Some matrix elements also depend on $\boldsymbol{k}$ orientation (or $e_i^{(3)} = k_i/k$).

In addition to pure solenoidal coupling terms $m_{\alpha\beta}$, which are the same as in solenoidal RDT, and to 'acoustical' or 'pseudo-sound' terms m_{34}, m_{43}, which correspond to Eq. (56), very interesting terms are

$$m_{\alpha 3} = e_i^{(\alpha)}(A_{ij} - A_{ji})e_j^{(3)}.$$

These terms represent a feedback from the dilatational mode to the solenoidal modes, and they are generated by the *rotational part* of the mean flow.

As an immediate consequence, the solenoidal flow is decoupled in the presence of an irrotational straining process. A second, less obvious, consequence, is that the kinetic energy growth rate is larger in compressible RDT than in solenoidal RDT, since the kinetic energy of the dilatational mode, allways positive, is just added to the kinetic energy of the solenoidal mode, which is independent of compressibility in this context. More generally, as firstly demonstrated by Jacquin *et al.* [46], the kinetic energy growth rate increases monotonically with increasing distortion Mach number M_d, from solenoidal RDT to 'pressure released' (very simple) RDT. One can retain that compressibility is allways shown as destabilizing regarding RDT for irrotational mean flow. A similar non-conventional behaviour is found in the case of pure plane shear, but only at moderate elapsed time ($St < 4$), as shown on Fig. 16 and 17. At larger time, the conventional 'stabilizing' behaviour is found. It is therefore clear that this stabilizing behaviour is explained by the presence of the $m_{\alpha 3}$ coupling terms, at least in the linear limit. Fig. 16 and 17 shows the main part of the turbulent kinetic energy growth rate Λ in Eq. (46), which reduces to $-2b_{12}$, ignoring other terms, as justified by [48,44].

More accurately, additional important equations for the compressible shear flow case are

$$\dot{(ku^{(2)})} = -S\frac{K_1}{K_\perp}y, \tag{58}$$

the equation for the solenoidal poloidal mode, in which the feedback from the dilatational mode involve y, as

$$y = \frac{\dot{z}}{k^2},$$

z being itself a rescaled pressure term satisfying the equation

$$\dot{\left(\frac{\dot{z}}{k^2}\right)} = c^2(z^{(s)} - z). \tag{59}$$

as in [44], $z = u^{(4)}(\mathbf{k},t)/(J(t)c(t)) = \imath\hat{p}/(Jc^2)$, (in the most general case), with $z^{(s)} = m_{3\alpha}u^{(\alpha)}/(Jkc^2)$, giving the incompressible limit $z = z^{(s)}$, equivalent to $\hat{p} = \hat{p}^{(s)}$ from the Poisson equation in Fourier space.

Going back to the (generally expected) stabilizing effect of compressibility, it is generally accepted, following Sarkar [48], that the weakening of pressure correlation is the only explanation. In fact, the weakening of pression can be demonstrated from the solution of the equation (59), under a scalar Green's function for pressure to velocity

$$z(\mathbf{k},t) = \int_{t_0}^{\infty} \mathcal{G}(\mathbf{k},t,t')z^{(s)}(\mathbf{k},t')dt'.$$

Recently, Thacker *et al.* [47] proposed an analytical solution for a similar scalar Green's function in the case of pure shear, generalizing the form $\mathcal{G} = \frac{\sin(ak(t-t'))}{ak}$ recovered in the shearless case (e.g. Pantano & Sarkar [49]).

We think that the explanation based on Eq. (59) is only a part of the whole story. This equation is also a byproduct of our general linear study based on the full system of linear equations. Conventional explanation is valid, for instance for accounting for the difference of the less compressible case in Fig. 16 (almost constant production rate at largest St), which is also a fully nonlinear result, and the pressure released case (curve in full line in Fig. 17). This 'explanation' is irrelevant when the curve of compressible RDT at large M_d and large elapsed time is found below the incompressible RDT limit curve (full line in Fig. 17), in contrast with our explanation based on equation (58). As a final remark, let us recall that the argument on the weakening of pressure is allways relevant in the irrotational 'mean' case, or at $St < 4$ in the shear case, but yields a *systematic destabilizing effect* because the pressure-released limit is allways over the incompressible RDT limit !

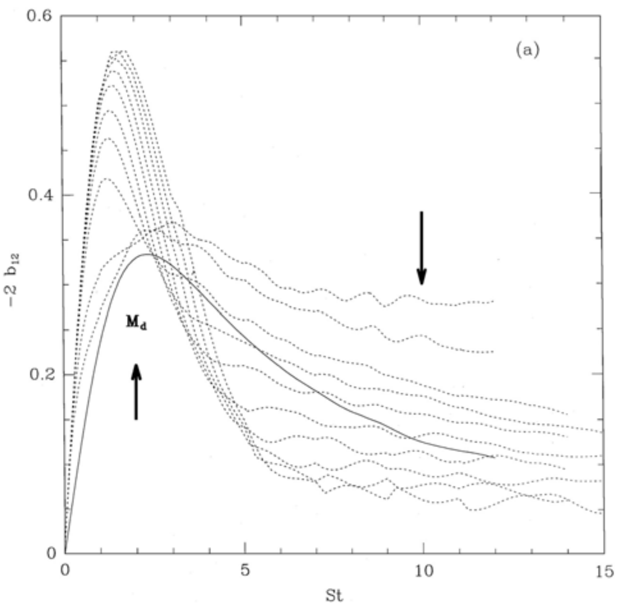

Fig. 16. Nondimensional production term, related to turbulent kinetic energy growth rate, full DNS.[44]

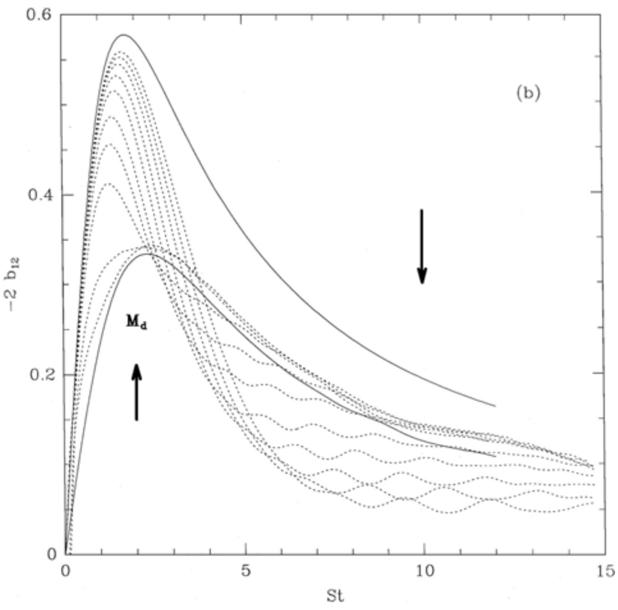

Fig. 17. Nondimensional production term, same conditions as on Fig. 16, linear quasi-isentropic compressible solution, so called (improperly) RDT. [44]

9 Conclusion and perspectives

Some cross-fertilization of ideas and methods is expected, comparing the different flow cases addressed here. Wave-Turbulence and turbulence with waves appeared in various domain. In the absence of waves, for instance for the case of homogeneous turbulence in the presence of pure plane shear, nonlinear spectral closures continue to present a challenge. Double diffusivity cannot be ignored in the linear MHD régime, probably in contrast with stably-stratified and weakly compressible flow cases. The 'dumbell argument', straighforward in MHD, was also successfully used in rotating turbulence [52]. In addition to these examples, the following points will be discussed, in the final version:

(1) Importance of detailed anisotropy (except in subsection 8.2), especially directional anisotropy.
(2) Good agreement between statistical theory and high resolution DNS (rotating and/or stratified turbulence).

(3) Statistical theory versus stability analysis ? Cyclonic/anticyclonic asymmetry in flows dominated by rotation, horizontal layering in flows dominated by stable stratification.
(4) Single-time or two-time statistics ? Linear and nonlinear theories.
(5) Connection with the ‘linear response approach’ of Kaneda and coworkers [12]
(6) How improving the eddy damping (ED) when it is needed ? Is allways ED unimportant in wave-turbulence theory ? [51,11]
(7) Towards inhomogeneous flows. WKB linear solutions.

BIBLIOGRAPHY

[1] G. K. Batchelor, The theory of homogeneous turbulence, Cambridge University Press, 1953.

[2] C. Cambon, J. F. Scott, ”Linear and nonlinear models of anisotropic turbulence,” Annu. Rev. Fluid Mech., vol. 31, pp. 1–53, 1999.

[3] C. Cambon, R. Rubinstein, ”Anisotropic developments for homogeneous shear flows,” Phys. Fluids, submitted.

[4] S. Kassinos, W. C. Reynolds, M. Rogers, “One-point turbulence structure tensors,” J. Fluid Mech., vol. 428, pp.213-248, 2000.

[5] I. Arad, V. S. L’vov, I. Procaccia, “Correlation functions in isotropic and anisotropic turbulence: the role of the symmetry group,” Phys. Rev. E, vol. 59, pp. 6753–6765, 1999.

[6] Written reports by Craya, Ph. D and P.S.T, in French, being unavailable or too abridged, more information can be obtained from the author upon request.

[7] J. R. Herring, “Approach of axisymmetric turbulence to isotropy,” Phys. Fluids, vol. 17, pp. 859–872, 1974.

[8] A. A. Townsend, The structure of turbulent shear flow, Cambridge University Press, 1956/1976.

[9] A. D. D.. Craik, W. O. Criminale, “ Evolution of wavelike disturbances in shear flows: a class of exact solutions of Navier-Stokes equations,” Proc. R. Soc. London Ser. A, vol. 406, pp. 13–26, 1986.

[10] S. A. Orszag, “ Analytical theories of turbulence,” J. Fluid Mech., vol. 41, pp. 363, 1970.

[11] Y. Kaneda, “Lagrangian Renormalized Approximation of Turbulence,” Fluid Dynamic Research, to appear, 2006.

[12] Y. Kaneda, present conference, keynote lecture.

[13] C. Cambon and L. Jacquin, “Spectral approach to non-isotropic turbulence subjected to rotation,” J. Fluid Mech., vol. 202, pp. 295–317, 1989.

[14] F. Waleffe, “Inertial transfers in the helical decomposition,” Phys. Fluids A, vol. 5, pp. 677–685, 1993.

[15] W.J. T. Bos, J. -P. Bertoglio, “Dynamics of spectrally truncated inviscid turbulence,” Phys. Fluids, submitted.

[16] M. Brachet, GDR turbulence, ESPI, Paris, France, Nov. 26, 2005.

[17] W. J. T. Bos, J. -P. Bertoglio, “A single-time two-point closure based on fluid particle displacements,” Phys. Fluids, vol. 18, accepted for publication.

[18] F. S. Godeferd, L. Lollini, “DNS of turbulence with confinment and rotation,” J. Fluid Mech., vol. 393, pp. 257–308, 1999.

[19] H. P. Greenspan, The theory of rotating fluids, Cambridge University Press, 1968.

[20] C. Cambon, N. N. Mansour, F. S. Godeferd, “Energy transfer in rotating turbulence,” J. Fluid Mech., vol. 337, pp. 303–332, 1997.

[21] F. Bellet, F. S. Godeferd, J. F. Scott and C. Cambon, “Wave-turbulence in rapidly rotating flows,” J. Fluid Mech., under press.

[22] S. Galtier, “A weak inertial wave-turbulence theory,” Phys. Rev. E, vol. 68, pp. 1–4, 2003.

[23] C. Cambon, R. Rubinstein, F. S. Godeferd, “Advances in wave-turbulence: rapidly rotating flows, New Journal of Physics, vol. 6, pp. 73, 2004.

[24] L. Jacquin, O. Leuchter, C. Cambon, J. Mathieu, “Homogeneous turbulence in the presence of rotation,” J. Fluid Mech., vol. 220, pp. 1–52, 1990.

[25] P. Bartello, O. Métais and M. Lesieur, “Coherent structures in rotating three-dimensional turbulence,” J. Fluid Mech., vol. 273, pp. 1–29, 1994.

[26] C. Morize, F. Moisy and M. Rabaud, “Decaying grid-generated turbulence in a rotating tank,” Phys. Fluids, vol. 17, 9, 095105, 2005.

[27] J.-N. Gence and C. Frick, C. R. Acad. Sci. Paris, vol. 329, Série II b, pp.351, 2001.

[28] J.-N. Gence and C. Frick, C. R. Acad. Sci. Paris, vol. 329, Série II b, pp.351, 2001.

[29] P. A. Davidson, P. J. Stapelhurst, S. B. Dalziel, “On the evolution of eddies in a rapidly rotating system,” J. Fluid Mech., to appear, 2006.

[30] L. Liechtenstein, F. S. Godeferd and C. Cambon, “Nonlinear formation of structures in rotating stratified turbulence,” Journal of Turbulence, Vol. 6, 1–18, 2005.

[31] F. S. Godeferd and C. Cambon, “Detailed investigation of energy transfers in homogeneous stratified turbulence,” Phys. Fluids, vol. 6, pp. 284–2100, 1994.

[32] J. J. Riley, R. W. Metcalfe, M. A. Weissman, “DNS of homogeneous turbulence in density-stratified fluids, in Proc. of AIP Conference on Nonlinear Properties of Internal Waves, B. J. West Editor, pp. 79–112, New York, American Institute of Physics, 1981.

[33] F. S. Godeferd, C. Staquet, “ Statistical modelling and DNS of decaying stably-stratified turbulence, Part II: Large and small-scale anisotropy,” J. Fluid Mech., vol. 486, pp. 115–159, 2003.

[34] L. Liechtenstein. Unpublished.

[35] P. Billant and J.-M. Chomaz, Phys. Fluids, vol. 13, pp. 1645–1651, 2001.

[36] E. Lindborg, “The energy cascade in a strongly stratified fluid,” J. Fluid Mech., vol. 550, pp. 207–242, 2006.

[37] J. G. Charney, “Geostrophic turbulence,” J. Atmos. Sci., vol. 28, pp. 1087–1085, 1971.

[38] J. R. Herring, J. Atmos. Sci., vol. 37, pp. 969–977, 1980.

[39] L. M. Smith, F. Waleffe, “Generation of slow large-scales in forced rotating stratified turbulence,” J. Fluid Mech., vol. 451, pp. 145–168, 2002.

[40] J. M. Lee, J. Kim, P. Moin, “Structure of turbulence at high shear rate,” J. Fluid Mech., vol. 216, pp. 561–583, 1990.

[41] K. Moffatt, J. Fluid Mech., vol. 28, 3, pp. 571–592, 1967.

[42] T. Alboussière, GDR dynamo, ENSL, Lyon, France, March 27, 2006.

[43] S. Galtier, S. Nazarenko, A. C. Newell, A. Pouquet, “A weak turbulence theory for incompressible MHD,” J. Plasma Physics, vol. 63, pp. 447–488, 2000.

[44] A. Simone, G. N. Coleman, C. Cambon, “The effect of compressibility in turbulent shear flow: a RDT and DNS study,” J. Fluid Mech. vol. 330, pp. 307–338, 1997.

[45] G. Fauchet, L. Shao, R. Wunenberger, J. -P Bertoglio, “An improved two-point closure for weakly compressible turbulence,” 11 Symp. Turb. Shear Flow, Grenoble, Sept. 8–10, 1997.

[46] L. Jacquin, C. Cambon, E. Blin, “Turbulence amplification by a shock wave and Rapid Distortion Theory,” Phys. Fluids A, vol. 10, pp. 2539–2550, 1993.

[47] W. D. Thacker, S. Sarkar, T. B. Gatski, “Analyzing the influence of compressibility on the rapid pressure-strain rate correlation in turbulent shear flow,” TSFP4 meeting and TCFD journal, submitted.

[48] S. Sarkar, “The stabilizing effect of compressibility in turbulent shear flows,” J. Fluid Mech., vol. 282, pp. 163–286, 1995.

[49] C. Pantano, S. Sarkar, “A study of compressibility effects in the high-speed turbulent shear layer using DNS,” J. Fluid Mech., vol. 451, pp. 329–371, 2002.

[50] Cambon, C., F. S. Godeferd, F. Nicolleau, J. C. Vassilicos, “Turbulent diffusion in rapidly rotating flows with and without stable stratification,” J. Fluid Mech., vol. 499, pp. 231–255, 2004.

[51] D. J. Benney, A. C. Newell, “Random Wave Closure,” Studies in Applied Math., vol. 48, 1969.

[52] K. Dang, P. Roy, “Numerical simulation of homogeneous turbulence,” Proc. Workshop on Macroscopic Modelling of Turbulent Flows and Fluid Mixtures. Springer, 1985.